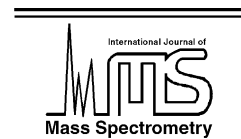




ELSEVIER

International Journal of Mass Spectrometry 225 (2003) 273–275



www.elsevier.com/locate/ijms

## Subject index Volume 225

### Ab initio calculations

The isobaric ions  $\text{CH}_3\text{O}-\text{P}=\text{O}^{\bullet+}$  and  $\text{CH}_3\text{O}-\text{P}-\text{NH}_2^+$  and their neutral counterparts: a tandem mass spectrometry and CBS-QB3 computational study, 11

### Acephate (*O,S*-dimethyl acetylphosphoramidothioate)

The isobaric ions  $\text{CH}_3\text{O}-\text{P}=\text{O}^{\bullet+}$  and  $\text{CH}_3\text{O}-\text{P}-\text{NH}_2^+$  and their neutral counterparts: a tandem mass spectrometry and CBS-QB3 computational study, 11

### Anion binding

Nano electrospray MS and MS–MS investigation of two polydentate Lewis acids,  $(\text{C}_6\text{F}_4\text{Hg})_3$  and *o*- $\text{C}_6\text{F}_4(\text{HgCl})_2$ , characterization and halide binding selectivity, 225

### Atmospheric chemistry

Electron-impact ionization of NO, NO<sub>2</sub>, and N<sub>2</sub>O, 25

### Blackbody infrared cooling

Experimental calibration of the SORI-CID internal energy scale: energy uptake and loss, 71

### Bond energies

Electron impact ionization of cobalt-tricarbonyl-nitrosyl, cyclopentadienyl-cobalt-dicarbonyl and biscyclopentadienyl-cobalt: appearance energies, bond energies and enthalpies of formation, 115

### Breakdown

Near-threshold photoionization spectroscopy of the mono-terpenes limonene and carvone, 261

### CBS-QB3

The isobaric ions  $\text{CH}_3\text{O}-\text{P}=\text{O}^{\bullet+}$  and  $\text{CH}_3\text{O}-\text{P}-\text{NH}_2^+$  and their neutral counterparts: a tandem mass spectrometry and CBS-QB3 computational study, 11

### Cesium clusters

Useful yields of  $\text{MCs}_x^+$  clusters: a cesium concentration-dependent study on the Cation Mass Spectrometer (CMS), 135

### Cesium concentration

Useful yields of  $\text{MCs}_x^+$  clusters: a cesium concentration-dependent study on the Cation Mass Spectrometer (CMS), 135

### CID MS–MS

Nano electrospray MS and MS–MS investigation of two polydentate Lewis acids,  $(\text{C}_6\text{F}_4\text{Hg})_3$  and *o*- $\text{C}_6\text{F}_4(\text{HgCl})_2$ , characterization and halide binding selectivity, 225

### Classical trajectory

Development of classical trajectory methodology for the study of dissociation dynamics of polyatomic ions, 191

### Combustion

Electron-impact ionization of NO, NO<sub>2</sub>, and N<sub>2</sub>O, 25

### Continuous ion introduction

Time-of-flight (TOF) mass spectrometer without pulses of any kind, with continuous ion introduction, 101

### Cross-sections

Electron-impact ionization of NO, NO<sub>2</sub>, and N<sub>2</sub>O, 25

### Dehydration

Chemistry in aldol complexes of metal dications: dehydration of the bisligand species, 155

### Diffusion losses

Comparison of the planar and coaxial field asymmetrical waveform ion mobility spectrometer (FAIMS), 39

### Dissociation

Electron capture induced dissociation of peptide dications, 83

### Dissociation energies

Electron impact ionization of cobalt-tricarbonyl-nitrosyl, cyclopentadienyl-cobalt-dicarbonyl and biscyclopentadienyl-cobalt: appearance energies, bond energies and enthalpies of formation, 115

### Double spiking

A preliminary study of isotope fractionation in molybdenites, 177

### Electron bombardment

High temperature Langmuir vaporization mass spectrometer, 1

### Electron capture

Electron capture induced dissociation of peptide dications, 83

### Electron-impact ionization

Electron-impact ionization of NO, NO<sub>2</sub>, and N<sub>2</sub>O, 25

### Electron–molecule ionization cross-sections

Absolute partial and total electron-impact ionization cross-sections of the  $\text{CCl}_2\text{F}_2$  molecule, 127

### Electrospray ionization

Chemistry in aldol complexes of metal dications: dehydration of the bisligand species, 155

### FAIMS

Comparison of the planar and coaxial field asymmetrical waveform ion mobility spectrometer (FAIMS), 39

### Femtosecond ionization

Femtosecond ionization and dissociation of laser desorbed nitro-PAHs, 53

- Field ionization  
 Multielectron dissociative ionization of  $\text{CH}_3\text{I}$  under strong picosecond laser irradiation, 249
- Focusing  
 Comparison of the planar and coaxial field asymmetrical waveform ion mobility spectrometer (FAIMS), 39
- Fourier transform laser microprobe mass spectrometry  
 Molecular speciation of inorganic mixtures by Fourier transform laser microprobe mass spectrometry, 213
- Fourier transformation  
 Time-of-flight (TOF) mass spectrometer without pulses of any kind, with continuous ion introduction, 101
- Fragmentation  
 Near-threshold photoionization spectroscopy of the mono-terpenes limonene and carvone, 261
- Gas-phase enthalpies of formation  
 Electron impact ionization of cobalt-tricarbonyl-nitrosyl, cyclopentadienyl-cobalt-dicarbonyl and biscyclopentadienyl-cobalt: appearance energies, bond energies and enthalpies of formation, 115
- Glycine  
 Gas-phase  $\text{Cu}^+$ - and  $\text{Ag}^+$ -glycine complexes produced with a new source, 89
- High temperature mass spectrometry  
 High temperature Langmuir vaporization mass spectrometer, 1
- Hybrid DFT method  
 Hybrid DFT study on the gas-phase  $\text{S}_{\text{N}}2$  reactions at neutral oxygen, 167
- Inorganic salts  
 Molecular speciation of inorganic mixtures by Fourier transform laser microprobe mass spectrometry, 213
- Internal energy deposition  
 Experimental calibration of the SORI-CID internal energy scale: energy uptake and loss, 71
- Ion dissociation dynamics  
 Development of classical trajectory methodology for the study of dissociation dynamics of polyatomic ions, 191
- Ion mobility  
 Comparison of the planar and coaxial field asymmetrical waveform ion mobility spectrometer (FAIMS), 39
- Ion solvation  
 Chemistry in aldol complexes of metal dications: dehydration of the bisligand species, 155
- Ionization energy  
 Near-threshold photoionization spectroscopy of the mono-terpenes limonene and carvone, 261
- Ionization probability  
 Useful yields of  $\text{MCs}_x^+$  clusters: a cesium concentration-dependent study on the Cation Mass Spectrometer (CMS), 135
- Isotope fractionation  
 A preliminary study of isotope fractionation in molybdenites, 177
- Kinetic energy release distribution  
 Theoretical calculation of isotope effects, kinetic energy release and effective temperatures for alkylamines, 233
- Kinetic isotope effect  
 Theoretical calculation of isotope effects, kinetic energy release and effective temperatures for alkylamines, 233
- Langmuir vaporization  
 High temperature Langmuir vaporization mass spectrometer, 1
- Laser desorption  
 Femtosecond ionization and dissociation of laser desorbed nitro-PAHs, 53
- Low temperature mass spectrometry  
 Experimental calibration of the SORI-CID internal energy scale: energy uptake and loss, 71
- Mass spectra  
 Electron impact ionization of cobalt-tricarbonyl-nitrosyl, cyclopentadienyl-cobalt-dicarbonyl and biscyclopentadienyl-cobalt: appearance energies, bond energies and enthalpies of formation, 115
- Mass spectrometer  
 Gas-phase  $\text{Cu}^+$ - and  $\text{Ag}^+$ -glycine complexes produced with a new source, 89
- Mass spectrometry  
 A preliminary study of isotope fractionation in molybdenites, 177  
 Multielectron dissociative ionization of  $\text{CH}_3\text{I}$  under strong picosecond laser irradiation, 249
- Metal cations  
 Chemistry in aldol complexes of metal dications: dehydration of the bisligand species, 155
- Metal-amino acid complexes  
 Gas-phase  $\text{Cu}^+$ - and  $\text{Ag}^+$ -glycine complexes produced with a new source, 89
- Metastable ion decay  
 Electron impact ionization of cobalt-tricarbonyl-nitrosyl, cyclopentadienyl-cobalt-dicarbonyl and biscyclopentadienyl-cobalt: appearance energies, bond energies and enthalpies of formation, 115
- Methamidophos (*O,S*-dimethylphosphoramidothiolate)  
 The isobaric ions  $\text{CH}_3\text{O}-\text{P}=\text{O}^{\bullet+}$  and  $\text{CH}_3\text{O}-\text{P}-\text{NH}_2^+$  and their neutral counterparts: a tandem mass spectrometry and CBS-QB3 computational study, 11
- Mobility dependence  
 Comparison of the planar and coaxial field asymmetrical waveform ion mobility spectrometer (FAIMS), 39
- Molecular speciation  
 Molecular speciation of inorganic mixtures by Fourier transform laser microprobe mass spectrometry, 213
- Molybdenites  
 A preliminary study of isotope fractionation in molybdenites, 177
- Molybdenum  
 A preliminary study of isotope fractionation in molybdenites, 177

- Multiple ionization  
Femtosecond ionization and dissociation of laser desorbed nitro-PAHs, 53
- Multiply charged ions  
Chemistry in aldol complexes of metal dications: dehydration of the bisligand species, 155  
Multielectron dissociative ionization of  $\text{CH}_3\text{I}$  under strong picosecond laser irradiation, 249
- Nanoelectrospray  
Nanoelectrospray MS and MS–MS investigation of two polydentate Lewis acids,  $(\text{C}_6\text{F}_4\text{Hg})_3$  and  $o\text{-C}_6\text{F}_4(\text{HgCl})_2$ , characterization and halide binding selectivity, 225
- Near-threshold  
Near-threshold photoionization spectroscopy of the mono-terpenes limonene and carvone, 261
- Neutralization–reionization mass spectrometry  
The isobaric ions  $\text{CH}_3\text{O–P=O}^+$  and  $\text{CH}_3\text{O–P–NH}_2^+$  and their neutral counterparts: a tandem mass spectrometry and CBS-QB3 computational study, 11
- Nitro-PAHs  
Femtosecond ionization and dissociation of laser desorbed nitro-PAHs, 53
- $\text{NO}_x$   
Electron-impact ionization of  $\text{NO}$ ,  $\text{NO}_2$ , and  $\text{N}_2\text{O}$ , 25
- Nozzle-skimmer fragmentation  
Nanoelectrospray MS and MS–MS investigation of two polydentate Lewis acids,  $(\text{C}_6\text{F}_4\text{Hg})_3$  and  $o\text{-C}_6\text{F}_4(\text{HgCl})_2$ , characterization and halide binding selectivity, 225
- Numerically induced chaos  
Development of classical trajectory methodology for the study of dissociation dynamics of polyatomic ions, 191
- Partial ionization cross-sections  
Absolute partial and total electron-impact ionization cross-sections of the  $\text{CCl}_2\text{F}_2$  molecule, 127
- Peptides  
Electron capture induced dissociation of peptide dications, 83
- Photoelectron spectroscopy  
Near-threshold photoionization spectroscopy of the mono-terpenes limonene and carvone, 261
- Pollution control  
Electron-impact ionization of  $\text{NO}$ ,  $\text{NO}_2$ , and  $\text{N}_2\text{O}$ , 25
- Polydentate Lewis acid  
Nanoelectrospray MS and MS–MS investigation of two polydentate Lewis acids,  $(\text{C}_6\text{F}_4\text{Hg})_3$  and  $o\text{-C}_6\text{F}_4(\text{HgCl})_2$ , characterization and halide binding selectivity, 225
- Quantification  
Useful yields of  $\text{MCs}_x^+$  clusters: a cesium concentration-dependent study on the Cation Mass Spectrometer (CMS), 135
- Reaction mechanism  
Hybrid DFT study on the gas-phase  $\text{S}_{\text{N}}2$  reactions at neutral oxygen, 167
- Scaling  
Development of classical trajectory methodology for the study of dissociation dynamics of polyatomic ions, 191
- Secondary Ion Mass Spectrometry  
Useful yields of  $\text{MCs}_x^+$  clusters: a cesium concentration-dependent study on the Cation Mass Spectrometer (CMS), 135
- Selectivity  
Nanoelectrospray MS and MS–MS investigation of two polydentate Lewis acids,  $(\text{C}_6\text{F}_4\text{Hg})_3$  and  $o\text{-C}_6\text{F}_4(\text{HgCl})_2$ , characterization and halide binding selectivity, 225
- Semi-quantification  
Molecular speciation of inorganic mixtures by Fourier transform laser microprobe mass spectrometry, 213
- SIMS  
High temperature Langmuir vaporization mass spectrometer, 1
- $\text{S}_{\text{N}}2$  at neutral oxygen  
Hybrid DFT study on the gas-phase  $\text{S}_{\text{N}}2$  reactions at neutral oxygen, 167
- SORI-CID FT-ICR  
Experimental calibration of the SORI-CID internal energy scale: energy uptake and loss, 71
- Strong laser fields  
Multielectron dissociative ionization of  $\text{CH}_3\text{I}$  under strong picosecond laser irradiation, 249
- Surface ionization  
High temperature Langmuir vaporization mass spectrometer, 1
- Tandem mass spectrometry  
The isobaric ions  $\text{CH}_3\text{O–P=O}^+$  and  $\text{CH}_3\text{O–P–NH}_2^+$  and their neutral counterparts: a tandem mass spectrometry and CBS-QB3 computational study, 11
- Time-of-flight  
Time-of-flight (TOF) mass spectrometer without pulses of any kind, with continuous ion introduction, 101
- Useful yield  
Useful yields of  $\text{MCs}_x^+$  clusters: a cesium concentration-dependent study on the Cation Mass Spectrometer (CMS), 135
- Work function shifts  
Useful yields of  $\text{MCs}_x^+$  clusters: a cesium concentration-dependent study on the Cation Mass Spectrometer (CMS), 135